Fatigue reliability analysis for structures with known loading trend

Zhen Hu[1], Xiaoping Du[1]*, Daniel Conrad[2], Ray Twohy[2], and Michael Walmsley[2]

1. Department of Mechanical and Aerospace Engineering, Missouri University of Science and Technology, Rolla, MO, USA, 65401

2. Division of Quality and Reliability, Hussmann Corporation, Bridgeton, MO, USA, 63044

*Corresponding author

Dr. Xiaoping Du

Associate Professor of Mechanical Engineering
Department of Mechanical and Aerospace Engineering
Missouri University of Science and Technology
400 West 13th Street, Toomey Hall 290D,
Rolla, MO 65401, U.S.A.
Tel: 1-573-341-7249
Fax: 1-573-341-4607
E-mail: dux@mst.edu

Abstract

Variations, such as those in product operation environment and material properties, result in random fatigue life. Variations in material fatigue properties depend on stochastic stress responses due to their nonlinear relationships with other random variables such as stochastic loading and dimensions. In this work, an efficient fatigue reliability analysis method is developed to accommodate those uncertainties for structures under cyclic loads with known loading trend. To reduce the computational cost, the method incorporates the fatigue life analysis model and the saddlepoint approximation method with the fast integration method. The new method is applied to the fatigue reliability analysis of a cantilever beam and a door cam. The results show high accuracy and efficiency of the proposed method benchmarked with Monte Carlo Simulations.

Keyword: Fatigue reliability; Stress-dependent; Monte Carlo Simulation; Cyclic load

1. Introduction

Fatigue life assessment is a critical issue during the design process for many products. Due to inherent uncertainties, fatigue life always varies around the designed fatigue life. It is desirable to assess the fatigue life probabilistically rather than deterministically. The most commonly used probabilistic assessment method is the fatigue reliability analysis, which provides the probability that the actual fatigue life is greater than a desired life.

Fatigue reliability analysis methods are classified into the following three categories:

- Strain-life based method [1, 2]

  The method predicts fatigue life according to the strain response, which is usually related to the initial crack.

- Stress-life based method [3-7]

  Fatigue life is evaluated based on the material S-N curve. The initiation and propagation of the crack are not differentiated from each other in the stress-life model. Only the total fatigue life is considered.

- Fracture mechanics method [3-7]

Fracture mechanics methods are used to estimate if a crack grows to a critical size. This method usually combines the strain-life method to estimate the crack initiation.

This work employs the stress-life based fatigue reliability analysis method, and the effects of uncertainties in the design variables and the S-N curve on the fatigue life are investigated. The relevant research is reviewed below.

In addition to aforementioned methods [8-10], other methods have also been proposed. For instance, Guo and Chen [3-7] developed a fatigue reliability analysis method for steel bridges based on the long-term stress monitoring. Liu [11] proposed an efficient time-dependent fatigue reliability analysis method by using the moment matching method and the First Order Reliability Method (FORM). A unimodal distribution characterized by four parameters was introduced by Low [12] in predicting the uncertainty in fatigue damage. To account for the correlation effect of fatigue reliability, a fast reliability assessment approach was proposed based on the detail fatigue rating method [13]. The Kriging and radial basis functions were applied to the fatigue reliability analysis of a wire bond structure by Rajaguru, et. al [14]. Baumert and Pierron [15] studied the implication of fatigue properties of batteries on the reliability of flexible electronics. To

overcome the expensive computational effort of Monte Carlo simulation (MCS), Norouzi and Nikolaidis [16] presented an efficient fatigue reliability analysis method for structures subjected to a dynamic load.

Many probabilistic models have also been developed to model the statistical characteristics of the S-N curve [17]. Studies of the S-N curve indicate that material fatigue properties are uncertain with stress-dependent characteristics [18-27]. Since stress responses are usually also uncertain, material fatigue properties are uncertain factors whose stochastic nature is governed by other uncertainties. The stress-dependent fatigue properties make the fatigue reliability analysis different from and more difficult than regular reliability analysis problems.

The stress-dependent uncertainty in fatigue properties has not been sufficiently considered in the majority of fatigue reliability analysis methods. A few studies, such as the two methods developed by Liu [28-35], have concentrated on the reliability analysis with the stress-dependent properties, and their accuracy and efficiency can be further improved. For instance, the assumption of known stress distribution in the methods can be released by relating the fatigue reliability with basic random design variables.

The objective of this work is to improve the accuracy and efficiency of fatigue reliability analysis for special problems where structures are under cyclic loads with known loading trend. This kind of problem is common in many applications, especially for mechanisms with cyclic motions [12], for example, the transmission shaft under periodic loadings [36, 37], cams with known motion trajectory, and linkage mechanisms. The new method can account for uncertainties in both design variables and stress-dependent uncertainties in material fatigue properties. With the saddlepoint approximation (SPA) [38, 39] imbedded in the fast integration

[40], the method can produce a quick and accurate solution. The information required (inputs) and the outcome of the method are summarized below.

Input:

- Distributions of random input variables (dimensions, loading, etc.) for stress responses
- Distributions of random fatigue material properties
- Cyclic loading trend

Outputs:

- The distribution of fatigue life
- Fatigue reliability

A review of the fatigue life analysis under known loading trend is given in Sec. 2, followed by uncertainty analysis for fatigue life in Sec. 3. Sec. 4 discusses the proposed method, whose numerical procedure is summarized in Sec. 5. Two numerical examples are presented in Sec. 6, and conclusions are made in Sec. 7.

2. Fatigue life analysis with known loading trend

This work is for structures under cyclic load with known loading trend. As shown in Fig. 1, the known loading trend means that the same trend of the load repeats cycle by cycle and that each cycle of the load is identical. As stress responses in one load cycle is predictable with a mathematical model or computer aided engineering (CAE) simulation model, the trend of the stress responses is also known. As mentioned previously, this assumption is applicable for many problems.
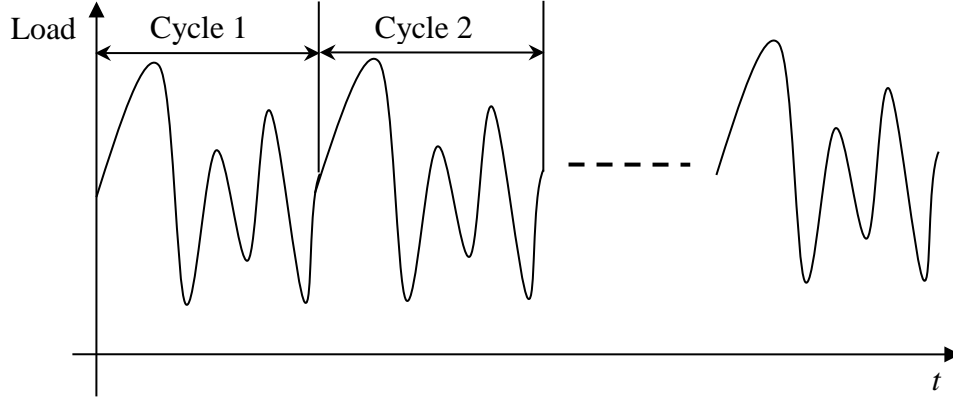
Fig. 1. Illustration of cyclic load with known loading trend

Many fatigue life prediction methods [41] and fatigue damage accumulation models [42-46] are available. We herein briefly review the fatigue life analysis model for structures with known loading trend.

Let $\mathbf{x} = [x_1, x_2, \cdots, x_n]$ be a vector of input variables to the nonlinear function or simulation model for stress responses as follows:

$$\mathbf{s}^o = g(\mathbf{x}) \tag{1}$$

where $g(\mathbf{x})$ is the stress responses function, and $\mathbf{s}^o = [s_1^o, s_2^o, \cdots, s_m^o]$ are blocks of stress responses in one cycle of the cyclic load. It should be noted that the left hand side of Eq. (1) is a vector because one cycle of the cyclic load may contain multiple loading peaks as can be seen in the numerical examples.

When the stress response is available and deterministic, the fatigue life analysis is straightforward. The most commonly used model is the Palmgren-Miner's rule [47-49], which is given by [50]

$$D = \sum_{i=1}^{m} \frac{n_i}{N_i} \tag{2}$$

where D is the accumulative fatigue damage, m is the number of stress blocks, n_i is the number of stress cycles at stress level s_i, and N_i is the number of cycles to failure at stress level s_i. N_i is obtained from the constant amplitude fatigue experiment.

In this work, we use the Palmgren-Miner's rule for fatigue damage analysis. However, other fatigue damage analysis methods can also be used with the proposed method. Since the fatigue experiments are conducted under constant amplitude loadings, the mean value corrections are usually applied before evaluating the fatigue damage using the Palmgren-Miner's rule [50]. Many empirical corrections were developed in the past decades. The most widely accepted corrections include the Goodman's and the Gerber's corrections. The two corrections relate the alternating stress amplitude to the mean stress response with the ultimate tensile strength [50].

For a general stress response s^o (a component of $\mathbf{s}^o$), the Goodman's correction is given by [51]

$$\frac{s_a}{s} + \frac{s_m}{s_u} = 1 \tag{3}$$

where s_u is the ultimate tensile strength, s is the stress response after correction, and s_a and s_m are the alternating stress amplitude and the mean stress, respectively, which are given by

$$s_a = \frac{s_{max}^o - s_{min}^o}{2} \tag{4}$$

and

$$s_m = \frac{s_{max}^o + s_{min}^o}{2} \tag{5}$$

in which s_{max}^o and s_{min}^o are the maximum and minimum values of s^o, respectively.

The Gerber's correction is [52]

6

$$\frac{S_a}{S} + \left(\frac{S_m}{S_u}\right)^2 = 1 \tag{6}$$

It is usually recommended that the Goodman correction is used for brittle materials and that

the Gerber's correction is used for ductile materials. After the mean value correction is made, the

number of cycles to failure at stress level s is then computed by

$$N = h(s) \tag{7}$$

where $h(s)$ is obtained from the S-N curve and is a function of stress level s.

With the Palmgren-Miner's rule, the fatigue life is estimated by

$$L_F = \frac{1}{1/N_1 + 1/N_2 + \cdots + 1/N_m} = \frac{1}{\sum\limits_{j=1}^{m} 1/N_j} \tag{8}$$

where L_F is the number of load cycles or fatigue life, and $\sum_{j=1}^{m} 1/N_j$ is the fatigue damage in

one cycle.

3. Uncertainty analysis of fatigue life

3.1.Uncertainties in stress responses

The fatigue life analysis model in Sec. 2 is in a deterministic form. In reality stress responses

from one product to another vary inevitably even if the design is the same. The stress variations

stem from variations in stress analysis input variables, for instance, stochastic loading,

manufacturing imprecision, and other noises in the operating environment.

We divide input variables into deterministic variables $\mathbf{d}$ and random variables $\mathbf{X}$. The stress

response is then presented by

$$\mathbf{S}^o = g(\mathbf{X}, \mathbf{d}) \tag{9}$$

Output variables $\mathbf{S}^o$ become random variables with distributions governed by the nonlinear function $g(\cdot)$ and the distributions of $\mathbf{X}$. The cumulative distribution function (CDF), or the probability that S^o, which is a component of $\mathbf{S}^o$, is less than a specific value s, is then computed by

$$\Pr\{S^o \le s\} = \int\limits_{S^0 \le s} f(\mathbf{x})d\mathbf{x} \tag{10}$$

in which $\Pr\{\cdot\}$ stands for a probability, and $f(\mathbf{x})$ is the joint probability density function (PDF) of $\mathbf{X}$.

3.2. Uncertainty in material fatigue properties

Uncertainty in material fatigue properties also results in uncertainty in fatigue life. The variations in material fatigue properties have been extensively studied [53]. For instance, the uncertainty of the fatigue crack growth model has been investigated [18-27], several probabilistic fatigue damage accumulation models have been developed [18-21], and models for probabilistic S-N curves have also been developed [22-25].

As the stress-life model is used in this work, we mainly consider variations in the S-N curve. In the past decades, many models were developed for describing the statistical nature of the S-N curve. The associated methods are classified into three groups - the statistical S-N curve [26, 27], the quantile S-N curve [28-31], and the stochastic S-N curve [32-34]. A detailed review about all the three groups can be found in [35].

What distinguishes the three groups is the way of handling correlations between stress levels. The statistical S-N curve assumes that the distributions of the cycle number at stress levels are independent while the quantile S-N curve assumes that they are dependent. The stochastic S-N

curve developed by Liu [35] releases the assumptions by modeling the dependence between stress levels using the Karhunen-Loeve (KL) expansion method [35]. We use the statistical S-N curve in this paper since the dependence between stress levels is not our focus and the dependent random variables can be transformed into independent ones using the Nataf transformation [54-56] or other methods, such as the method proposed by Noh, Choi, and Du [57, 58]. The developed method is also applicable for the other two groups of S-N curves.

What is in common between the three groups is that the number of cycles to failure under a stress level is a stress-dependent random variable. As a result, the mean and standard deviation of the number of cycles depend on stress levels [59, 60]. For a specific stress level s, the number of cycle, $N|s$ follows a Lognormal distribution or a Weibull distribution [33]. For the Lognormal distribution,

$$\frac{\log(N|s) - \mu_{\text{logN}}}{\sigma_{\text{logN}}} \sim N(0, 1^2) \tag{11}$$

where μ_{logN} and σ_{logN} are respectively the mean and standard deviation of $\log(N|s)$ and are given by

$$\mu_{\text{logN}} = h_1(s) \tag{12}$$

and

$$\sigma_{\text{logN}} = h_2(s) \tag{13}$$

in which $h_1(s)$ and $h_2(s)$ are functions of mean and standard deviation. These two functions are obtained based on the experimental testing data under the constant amplitude fatigue life testing. $N(\cdot, \cdot)$ stands for a normal distribution with the first parameter being the mean and the second parameter being the variance.

9

In the subsequent sections, the effect of the uncertainties on the fatigue life is analyzed. Based on the analysis, the new fatigue reliability analysis method is developed.

4. The proposed fatigue reliability analysis approach

4.1. Fatigue life reliability

Due to the uncertainties in the stress response and material fatigue properties, the fatigue life given in Eq. (8) is random. The CDF of the fatigue life L_F or the probability that L_F is less than a specific value l is given by

$$p_f = \Pr\{L_F < l\} = \Pr\left\{\frac{1}{1/(N_1|S_1) + 1/(N_2|S_2) + \cdots + 1/(N_m|S_m)} < l\right\} \tag{14}$$

where $N_i|S_i, i = 1, 2, \cdots, m$, are random numbers of cycles dependent on random stresses S_i given by

$$\mathbf{S} = [S_1, S_2, \cdots, S_m] = g_C(\mathbf{X}, \mathbf{d}) \tag{15}$$

in which $g_C(\cdot)$ is the stress response function after mean value correction on $\mathbf{S}^o = g(\mathbf{X}, \mathbf{d})$.

Eqs. (14) and (15) show that the fatigue life is a random variable and is a nonlinear function of random variables N_i whose distributions are dependent on S_i. Liu and Mahadevan [35] developed two methods for estimating the probability given in Eq. (14) when the distribution of S_i is known. The two methods include the moment-based method and FORM. Even though they can efficiently approximate the fatigue reliability given the stress distribution, there are still some limitations. The major limitation is to know the stress distribution, but it is usually unknown in the design stage. To obtain the distribution of the stress, we need to call Eq. (15) many times. If Eq. (15) involves CAE simulations, the computational cost will be high. As will be seen, the

method proposed in this work can cut the computational cost. To use the new method, we first transform the probability in Eq. (14) into

$$p_f = \Pr\{L_F < l\} = \Pr\{1/(N_1|S_1) + 1/(N_2|S_2) + \cdots + 1/(N_m|S_m) > 1/l\} \tag{16}$$

The distribution of N_i is dependent on S_i, which is governed by $g(\mathbf{X}, \mathbf{d})$. The fatigue probability of failure p_f depends on $\mathbf{X}$ as shown below.

$$p_f = \Pr\{L_F(\mathbf{X}, \mathbf{N}|\mathbf{X}) < l\} \tag{17}$$

where $\mathbf{N}|\mathbf{X} = [N_1|\mathbf{X}, N_2|\mathbf{X}, \cdots, N_m|\mathbf{X}]$ are random numbers of cycles dependent on $\mathbf{X}$.

In the following sections, we at first discuss the direct use of FORM and SORM for the fatigue reliability analysis. As will be seen, this treatment may not be accurate and efficient. We then present the new method, which improves both accuracy and efficiency. The comparison of the direct FORM/SORM and improved FORM/SORM are shown in the example section.

4.2. Direct FORM and SORM

One way of approximating the fatigue reliability is using FORM or SORM directly with the Rosenblatt transformation [12]. Before applying FORM or SORM, the most probable point (MPP), at which the joint probability density of random variables is the highest, needs to be identified. To determine the MPP, the dependent random variables $\mathbf{X}$ and $\mathbf{N}|\mathbf{X}$ are transformed into independent standard normal variables using the Rosenblatt transformation as follows [61]:

$$\mathbf{U_X} = \Phi^{-1}(F_{\mathbf{X}}(\mathbf{X}))$$

$$\mathbf{U_N} = \Phi^{-1}(F_{\mathbf{N}|\mathbf{X}}(\mathbf{N}|\mathbf{X})) \tag{18}$$

where $\Phi^{-1}(\cdot)$ is the inverse CDF of a standard normal variable, $F_{\mathbf{X}}(\cdot)$ is the CDF of random variable X_i, $F_{\mathbf{N}|\mathbf{X}}(\cdot)$ is the CDF of random variable $N_i|\mathbf{X}$ conditioned on $\mathbf{X}$, and $\mathbf{U_X}$ and $\mathbf{U_N}$

are independent standard normal variables corresponding to random variables $\mathbf{X}$ and $\mathbf{N} = [N_1, \cdots, N_m]$, respectively.

After the transformation, Eq. (17) becomes

$$p_f = \Pr\{L_F(\mathbf{U_X}, \mathbf{U_N}) < l\} = \Pr\{-1/L_F(\mathbf{U_X}, \mathbf{U_N}) < -1/l\} \tag{19}$$

The MPP $\mathbf{u}^*$ is then obtained by solving the following optimization model

$$\begin{cases} \min\limits_{\mathbf{u} = [\mathbf{u}_X, \mathbf{u}_N]} \|\mathbf{u}\| \\ \text{subject to} \\ -1/L_F(\mathbf{u_X}, \mathbf{u_N}) \le -1/l \end{cases} \tag{20}$$

in which $\|\cdot\|$ is the norm of a vector, and $1/L_F(\mathbf{u_X}, \mathbf{u_N})$ is given by

$$1/L_F(\mathbf{u_X}, \mathbf{u_N}) = 1/(N_1) + 1/(N_2) + \cdots + 1/(N_m) \tag{21}$$

where

$$N_i = F_{N_i|s_i}^{-1}(\Phi(\mathbf{u}_N)), i = 1, 2, \cdots, m \tag{22}$$

and

$$\mathbf{s} = [s_1, s_2, \cdots, s_m] = g_C(F_{X_1}^{-1}(\Phi(u_{X_1})), F_{X_2}^{-1}(\Phi(u_{X_2})), \ldots, F_{X_m}^{-1}(\Phi(u_{X_m})), \mathbf{d}) \tag{23}$$

in which $F_{N_i|s_i}^{-1}(\cdot)$ is the inverse CDF of $N_i|s_i$ conditional on s_i, and $F_{X_i}^{-1}(\cdot)$ is the inverse CDF of X_i.

Once the MPP $\mathbf{u}^*$ is available from Eq. (20), p_f is approximated using FORM as follows:

$$p_f = \Phi(-\beta) \tag{24}$$

where

$$\beta = \|\mathbf{u}^*\| \tag{25}$$

When the accuracy of FORM is not good, SORM can be employed. SORM is in general more accurate than FORM but is more computationally expensive than FORM as second derivatives are required. The Breitung's formulation for SORM is given by [61]

$$p_f = \Phi(-\beta) \prod_{i=1}^{m+n-1} (1 + \beta v_i)^{1/2} \tag{26}$$

where v_i ($i = 1, 2, \cdots, m+n-1$) are the principal curvatures of $-1 / L_F(\mathbf{U_X}, \mathbf{U_N})$ at the MPP. Details of SORM can be found in [62].

For n random variables in $\mathbf{X}$ and m stress responses in $\mathbf{S}$, there are totally $n+m$ variables in Eq. (20). Herein, the m stress responses in $\mathbf{S}$ are m different peak stresses in the dynamic stress responses. When m is large, the number of calling the stress response function in Eq. (15) will be high, and the efficiency will be low. In this work, we regard the situation that given a group of $\mathbf{x}$ and getting the corresponding m stresses as one function evaluation. The efficiency of direct use of FORM and SORM for reliability analysis can be improved. As will be seen in the example, the accuracy of the direct use of FORM may not be good either, and its accuracy also needs to be improved.

4.3. Proposed method

To overcome the drawbacks of the direct use of FORM or SORM, we propose a new method that integrates the fast integration method [61] and SPA [41]. The fatigue reliability introduced in Sec. 4.1 is computed with two steps: calculating the conditional fatigue reliability and calculating the unconditional fatigue reliability.

4.3.1. Conditional fatigue reliability analysis

The conditional fatigue reliability is based on the condition that random variables $\mathbf{X}$ are fixed at specific values $\mathbf{x}$, which lead to specific (deterministic) stress responses $\mathbf{s}$. The conditional probability of failure is then given by

$$p_f(\mathbf{x}) = \Pr\{L_F < l \mid \mathbf{X} = \mathbf{x}\} \tag{27}$$

or

$$p_f(\mathbf{x}) = \Pr\left\{ L_N = \frac{1}{L_F} = \sum_{i=1}^{m} \frac{1}{N_i \mid s_i} \geq \frac{1}{l} \,\middle|\, \mathbf{X} = \mathbf{x} \right\} \tag{28}$$

With the known values of $\mathbf{s}$, computing the above probability is just a traditional reliability analysis problem, and therefore existing methods, such as FORM, SORM, and SPA, can be used. In this work, we use SPA [40] because of the following reasons: (1) The limit-state function $\sum_{i=1}^{m} 1/(N_i \mid s_i)$ $(i=1,2,\ldots,m)$ in Eq. (28) is nonlinear with respect to random variables $N_i \mid s_i$ $(i=1,2,\ldots,m)$. The first order and second order approximations of the limit-state function may result in errors if FORM and SORM are used. (2) SPA treats the limit-state function $\sum_{i=1}^{m} 1/(N_i \mid s_i)$ $(i=1,2,\ldots,m)$ as a function of random variables $1/(N_i \mid s_i)$ $(i=1,2,\ldots,m)$, and the limit-state function becomes the sum of independent random variables and is therefore linear. There will be no error from the function approximation.

To use SPA, we first derive the Cumulant Generating Function (CGF) of $L_N = \sum_{i=1}^{m} 1/(N_i \mid s_i)$, which is given by

$$K_{L_N}(t) = \ln\left[\int_{-\infty}^{\infty} e^{t l_n} f_{L_N}(l_n)\,dl_n\right] \tag{29}$$

where $f_{L_N}(l_n)$ is the probability density function (PDF) of the random response L_N.

14

When $N_i|s_i$, $i=1, 2, \cdots, m$ are independent, we have

$$f_{L_N}(l_n) = f_{N_1|s_1}(n_1)f_{N_2|s_2}(n_2)\cdots f_{N_m|s_m}(n_m) \tag{30}$$

in which $f_{N_i|s_i}(n_i)$ is the PDF of $N_i|s_i$.

Substituting Eq. (30) into (29) yields

$$K_{L_N}(t) = \ln[\int_{-\infty}^{\infty} e^{t\sum_{i=1}^{m}1/(n_i|s_i)} f_{N_1|s_1}(n_1)f_{N_2|s_2}(n_2)\cdots f_{N_m|s_m}(n_m)dn_1 dn_2 \cdots dn_m] \tag{31}$$

Eq. (31) is rewritten as

$$K_{L_N}(t) = K_{N_1|s_1}(t) + K_{N_2|s_2}(t) + \cdots + K_{N_m|s_m}(t) \tag{32}$$

Directly evaluating Eq. (32) is very difficult. Herein, we use the power expansion of the CGF [40]. For $K_{N_i|s_i}(t)$, the power expansion is given by

$$K_{N_i|s_i}(t) = \sum_{j=1}^{\infty} \kappa_{i,j} \frac{t^j}{j!} \tag{33}$$

where $\kappa_{i,j}$ is the j-th cumulant of $N_i|s_i$.

If the first four cumulants are used, the cumulants $\kappa_{i,j}$, $j=1, 2, 3, 4$, are given in terms of moments as follows:

$$\begin{cases} \kappa_{i,1} = m_{i,1} \\ \kappa_{i,2} = m_{i,2} - m_{i,1}^2 \\ \kappa_{i,3} = 2m_{i,1}^3 - 3m_{i,1}m_{i,2} + m_{i,3} \\ \kappa_{i,4} = m_{i,4} - 4m_{i,1}m_{i,3} - 6m_{i,1}^4 + 12m_{i,1}^2 m_{i,2} - 3m_{i,2}^2 \end{cases} \tag{34}$$

in which $m_{i,j}$, $j=1, 2, 3$, and 4, are the first four moments about zero of $N_i|s_i$.

$m_{i,j}$, $j=1, 2, 3, 4$, are given by

$$m_{i,j} = \int_0^\infty \left(\frac{1}{n_i}\right)^j f_{N_i|S_i}(n_i)dn_i, \ \forall j=1, 2, 3, 4 \tag{35}$$

If higher order cumulants are used, the n-th order cumulant is given by

$$\kappa_{i,n} = m_{i,n} - \sum_{j=1}^{n-1}\binom{n-1}{j-1}k_{i,j}m_{i,n-j} \tag{36}$$

Plugging Eq. (33) into Eq. (32), we have

$$K_{L_N}(t) = \sum_{j=1}^\infty (\sum_{i=1}^m \kappa_{i,j})\frac{t^j}{j!} \tag{37}$$

Once the expressions of $K_{L_N}(t)$ are available, the saddlepoint is obtained by solving the following equation:

$$\frac{1}{l} = (\sum_{i=1}^m \kappa_{i,1}) + (\sum_{i=1}^m \kappa_{i,2})\frac{\eta}{1!} + (\sum_{i=1}^m \kappa_{i,3})\frac{\eta^2}{2!} + (\sum_{i=1}^m \kappa_{i,4})\frac{\eta^3}{3!} \tag{38}$$

With the saddlepoint η solved from Eq. (38), the conditional probability of failure is then calculated by [63]

$$p_f(\mathbf{x}) = \Pr\{L_N \geq \frac{1}{l}\Big|\mathbf{X}=\mathbf{x}\}$$
$$= 1 - \Phi(w) - \phi(w)(\frac{1}{w}-\frac{1}{v}) \tag{39}$$

in which

$$w = \text{sign}(\eta)\left\{2\left[\eta K'_{L_N}(\eta) - K_{L_N}(\eta)\right]\right\}^{1/2} \tag{40}$$

$$v = \eta\left[K''_{L_N}(\eta)\right]^{1/2} \tag{41}$$

$$K_{L_N}(\eta) = \sum_{j=1}^4 (\sum_{i=1}^m \kappa_{i,j})\frac{\eta^j}{j!} \tag{42}$$

$$\text{sign}(\eta) = \begin{cases} 1, \eta > 0 \\ 0, \eta = 0 \\ -1, \eta < 0 \end{cases} \tag{43}$$

where $\phi(\cdot)$ is the PDF of a standard normal variable, $K'_{L_N}(\eta)$ and $K''_{L_N}(\eta)$ are the first and second derivatives of $K_{L_N}(\eta)$, respectively.

The derivation of $K_{L_N}(t)$ is based on the condition that $N_i | s_i$, $i = 1, 2, \cdots, m$, are independent. It is the assumption for the statistical S-N curve we use in this work. When $N_i | s_i$, $i = 1, 2, \cdots, m$, are dependent (i.e. stochastic S-N curve), the dependent random variables should be transformed into independent random variables. Then, the dimension reduction method (DRM) can be applied to estimate $K_{L_N}(t)$ [40]. Once the $K_{L_N}(t)$ is available, Eqs. (37) through (43) are used to approximate the conditional probability of failure.

Note that, the above analysis only calls the stress analysis once.

4.3.2. Unconditional fatigue reliability analysis

The conditional probability of failure obtained in the last subsection is conditional on the stress or random variables $\mathbf{X}$. The unconditional probability of failure is given by

$$p_f = \int p_f(\mathbf{x}) f_{\mathbf{X}}(\mathbf{x}) d\mathbf{x} \tag{44}$$

Directly calculating the integral above is costly, especially when the dimension of $\mathbf{X}$ is high. To reduce the cost, following the same principle in Ref. [40], we introduce a new random variable $U_e \sim N(0, 1^2)$ such that

$$\Phi(u_{p_f}) = \Pr\{U_e \leq u_{p_f}\} = p_f(\mathbf{x}) \tag{45}$$

Then

$$u_{p_f} = \Phi^{-1}[p_f(\mathbf{x})] \tag{46}$$

Substituting Eq. (45) into Eq. (44) yields

$$p_f = \int \Pr\{U_e \le u_{p_f}\} f_{\mathbf{X}}(\mathbf{x}) d\mathbf{x} = \int \int_{U_e \le u_{p_f}} \phi(u_e) du_e f_{\mathbf{X}}(\mathbf{x}) d\mathbf{x} \tag{47}$$

Eq. (47) can be further written as

$$p_f = \Pr\{U_e \le u_{p_f}(\mathbf{X})\} = \Pr\{U_e - u_{p_f}(\mathbf{X}) \le 0\} \tag{48}$$

Combining Eq. (46) with Eq. (48), we have

$$p_f = \Pr\{U_e - \Phi^{-1}[p_f(\mathbf{X})] \le 0\} \tag{49}$$

To approximate the probability given in Eq. (49), we define a new limit-state function

$$g_{new}(U_e, \mathbf{X}) = U_e - \Phi^{-1}[p_f(\mathbf{X})] \tag{50}$$

If the FORM or SORM is employed, the MPP search is then given by

$$\begin{cases} \min_{\mathbf{u}=[u_e, \mathbf{u_X}]} \beta = \|\mathbf{u}\| \\ u_e - \Phi^{-1}[p_f(\mathbf{x})] \le 0 \end{cases} \tag{51}$$

in which a general component x of $\mathbf{x}$ is $x = F_x^{-1}[\Phi(u_X)]$, where u_X is a general component of $\mathbf{u_X}$.

After the MPP $\mathbf{u}^*$ is found, p_f is computed by FORM as follows

$$p_f = 1 - \Phi(\beta) = 1 - \Phi(\|\mathbf{u}^*\|) \tag{52}$$

If SORM is used to approximate Eq. (49), p_f is obtained by plugging $\mathbf{u}^*$ and the main curvatures of $g_{new}(U_e, \mathbf{X})$ at the MPP into Eq. (26). We called the two methods the improved FORM and improved SORM, respectively.

$m+n$ random variables exist if FORM or SORM is directly used as indicated in Eq. (20). With the proposed method, the number of random variables is reduced to $n+1$ as shown in Eq.

(51). The dimension reduction means less calls of the stress analysis, thereby less computational effort. As a result, the proposed method is more efficient than the direct use of FORM or SORM. The accuracy of the proposed method is also better than the direct use of FORM. The major reason is that the conditional probability obtained from SPA is accurate.

Since we use MCS as a benchmark for methodology evaluation, next, we briefly discuss how to use MCS for the fatigue reliability analysis.

4.4. Monte Carlo Simulation for fatigue reliability analysis

For MCS, let the number of samples be n_{MCS}. We first generate samples for the n independent variables $\mathbf{X}$, we then generate samples for $N_i, i = 1, 2, \cdots, m$. The two steps are used because $N_i, i = 1, 2, \cdots, m$ depend on $\mathbf{X}$. With the samples of $N_i, i = 1, 2, \cdots, m$, we generate n_{MCS} samples for L_F. The probability of failure is then estimated by

$$p_f^{MCS} = \frac{n_f}{n_{MCS}} \tag{53}$$

in which n_f is the number of samples that satisfy $L_F < l$.

5. Numerical procedure

Fig. 2 shows the numerical procedure for identifying the MPP. The procedure is explained in details below.
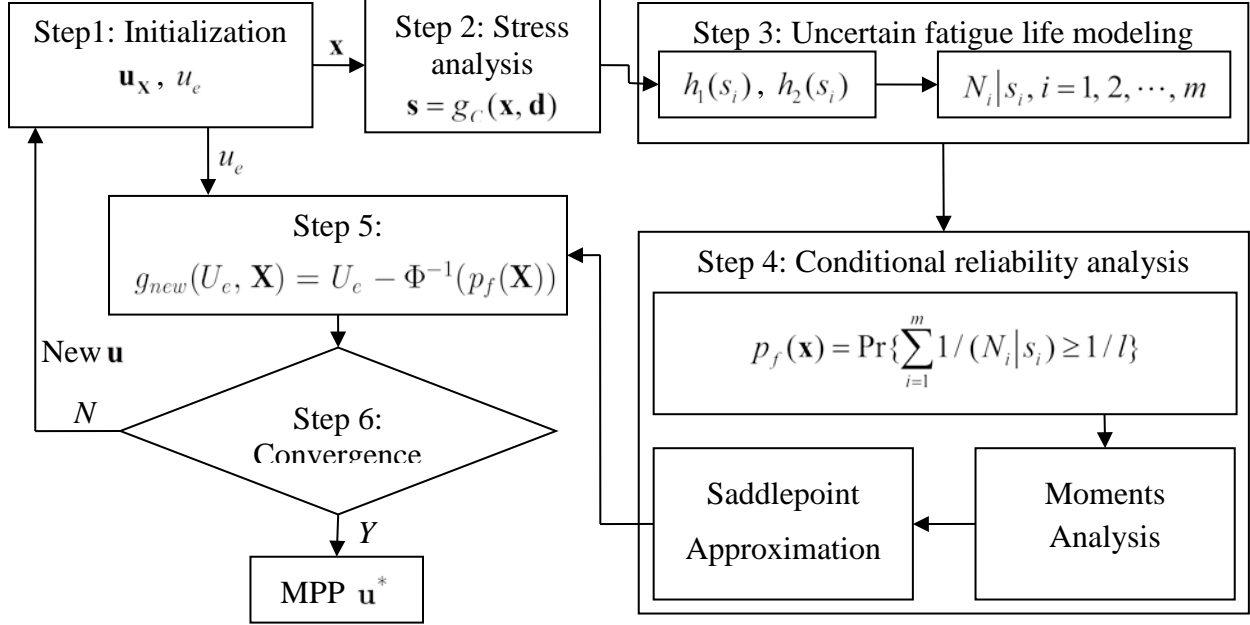
Fig. 2. Flowchart of MPP search

Step 1: Initialization: Set initial point $\mathbf{u} = [\mathbf{u}_X, u_e]$ for the MPP search.

Step 2: Stress analysis: For a given point $\mathbf{u}_X$ perform stress analysis using Eq. (15).

Step 3: Use the fatigue life model: Obtain the statistical parameters of the number of stress cycles, $N_i|s_i$, $i = 1, 2, \cdots, m$, with Eqs. (12) and (13).

Step 4: Conditional reliability analysis: Perform the conditional reliability analysis based on the information obtained in Step 3.

Step 5: Limit-state function evaluation: Transform the conditional probability of failure into the equivalent standard normal variable and evaluate the limit-state function in Eq. (50).

Step 6: Convergence check: If the reliability indexes β in two subsequent iterations are close enough, the MPP is identified and convergence is reached; then compute the probability of failure using FORM or SORM. Otherwise, generate a new point for $\mathbf{u}_X$ and u_e, and go to Step 2.

20

6. Numerical examples

Two numerical examples are presented to evaluate the proposed method.

6.1. A cantilever beam

As shown in Fig. 3, a cantilever beam is subjected to a random cyclic load F, which is plotted in Fig. 4. There are four blocks of load in each cycle of F. The peak values of the four blocks are F_1, F_2, F_3, and F_4, respectively. The corresponding valley value of each peak is zero.
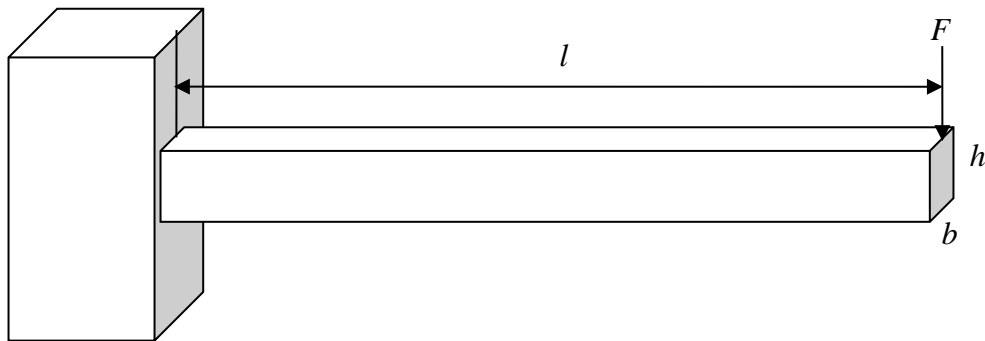
Fig. 3. A cantilever beam subjected to cyclic load
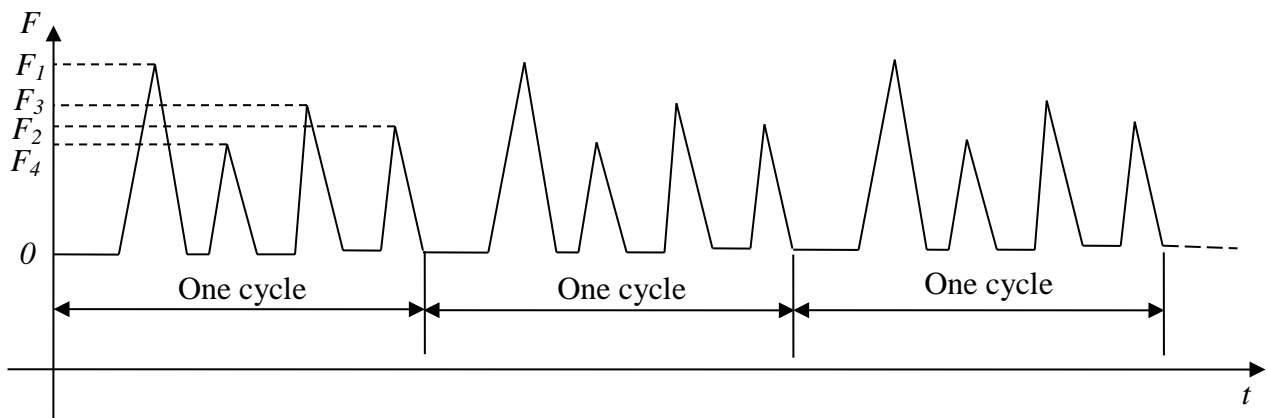
Fig. 4. Load trend over time

The maximum stresses $\mathbf{S}_{max}^{o}$ of the beam are given by

$$\mathbf{S}_{max}^{o} = [S_1^{o}, S_2^{o}, S_3^{o}, S_4^{o}] = \frac{6\mathbf{F}l}{bh^2} \tag{54}$$

where b, l, and h are the geometrical parameters as shown in Fig. 3 and $\mathbf{F} = [F_1, F_2, F_3, F_4]$ is the vector of forces in one cycle.

Since the corresponding valley of each peak of $\mathbf{F} = [F_1, F_2, F_3, F_4]$ is zero, we have

$$\mathbf{S}_{min}^{o} = [0, 0, 0, 0] \tag{55}$$

Eq. (54) implies that the stress response of the beam is proportional to the load on the beam. With the known trend of load over time, the trend of stress response is therefore known. Due to the uncertainties in the geometrical parameters, cyclic loading, and material fatigue properties, the fatigue life of the beam is also uncertain.

Since the material is brittle, the Goodman mean value correction is applied [41]. The corrected stress amplitude S_i, $i = 1, 2, 3, 4$, are given by

$$S_i = \frac{S_i^{o} S_u}{2S_u - S_i^{o}} \tag{56}$$

where S_u is the ultimate tensile strength of the material.

According to Eq. (8), the fatigue life of the beam presented in cycles is given by

$$L_F = \frac{1}{\sum_{i=1}^{4} 1/(N_i | S_i)} \tag{57}$$

in which $N_i | S_i, i = 1, 2, 3, 4$, are numbers of cycles to failure under the stress level S_i.

As discussed in Sec.3.2, $N_i | S_i$ is a stress-dependent random variable and follows a Log-normal distribution, defined by

$$\log(N_i \mid S_i) \sim N(\mu_{\log(N)}, \sigma^2_{\log(N)}) \tag{58}$$

$\mu_{\log(N)}$ and $\sigma_{\log(N)}$ are

$$\mu_{\log(N)} = \log\{10^{[c - d\log_{10}(S_i)]}\} \tag{59}$$

and

$$\sigma_{\log(N)} = 0.04\mu_{\log(N)} \tag{60}$$

where $c = 12.2$, and $d = 3.68$. The required fatigue life is $l = 1.5 \times 10^4$ cycles.

Table 1 gives the distributions of the random variables.

Table 1 Random variables

Variable	Mean Value	Standard Deviation	Distribution Type
l (in)	9	0.01	Normal
b (in)	0.2	0.005	Normal
h (in)	0.4	0.005	Normal
S_u (ksi)	221.7	5	Lognormal
F_1 (lb)	80	3	Lognormal
F_2 (lb)	60	2	Lognormal
F_3 (lb)	70	2	Lognormal
F_4 (lb)	65	2	Lognormal

There are eight random variables (i.e. l, b, h, S_u, F_1, F_2, F_3, and F_4) in the stress response function, and four random responses, S_i, i=1, 2, 3, 4, in the fatigue life function. The problem was solved by the direct FORM and SORM, the improved FORM and SORM, and MCS. For MCS, the numbers of samples was 3×10^6. The percentage error with respect to MCS is defined by

$$\varepsilon = \frac{\left| p_f - p_f^{MCS} \right|}{p_f^{MCS}} \times 100\% \tag{61}$$

where p_f^{MCS} is obtained from MCS while p_f is obtained from other methods.

Table 2 shows the results, including the MCS solution and the associated 95% confidence interval in brackets, and the number of function calls (NOF) of the stress response function, which is used as the measure of efficiency.

Table 2 Results of fatigue reliability analysis of a cantilever beam

Method	FORM	Improved FORM	SORM	Improved SORM	MCS	
p_f	0.0056	0.0096	0.0085	0.0096	0.0095	[0.0094, 0.0097]
Error (%)	41.32	1.06	10.67	1.06	-	
NOF	261	80	352	135	3×10^6	

The results show that the proposed method is more accurate and efficient than the direct FORM and SORM.

To study the robustness of the proposed method, we also performed reliability analyses at different failure levels using the direct FORM and SORM, the improved FORM and SORM, and MCS. The number of simulations of MCS is 3×10^6. The failure thresholds vary from 0.9×10^4 to 3.0×10^4. The results are given in Table 3 and plotted in Fig. 5. Table 4 presents the percentage errors of the four methods with respect to MCS. The percentage errors are also plotted in Fig. 6. The numbers of function calls are listed in Table 5 and plotted in Fig. 7.
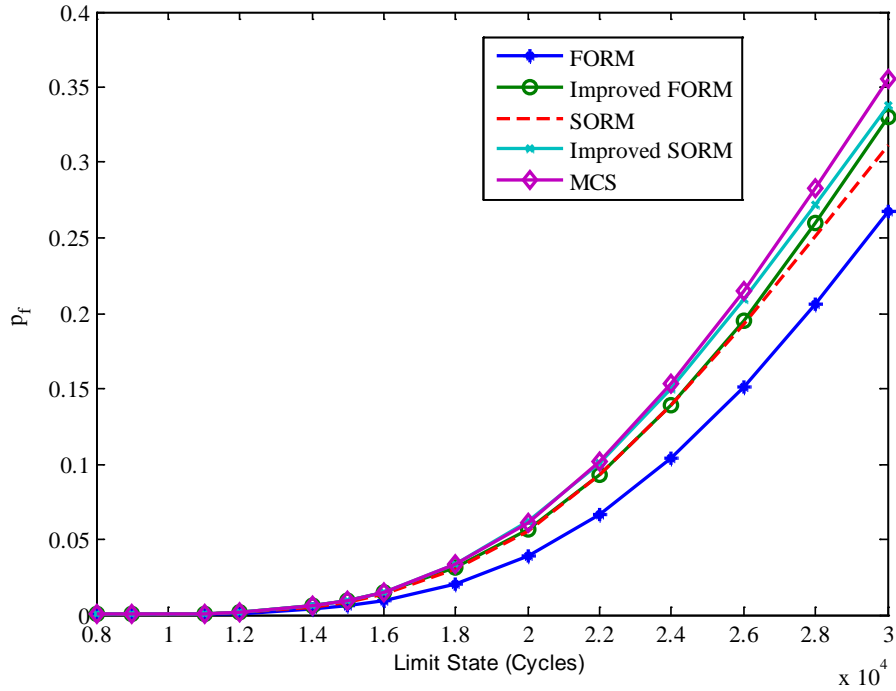
Fig. 5 Probability of failure under different failure levels

Table 3 Probabilities of failure at different failure levels

Limit State	p_f					
	FORM	Improved FORM	SORM	Improved SORM	MCS	
0.8×10^4	2.13×10^{-5}	2.78×10^{-5}	3.13×10^{-5}	2.95×10^{-5}	3.07×10^{-5}	$[2.44 \times 10^{-5},$ $3.69 \times 10^{-5}]$
0.9×10^4	6.89×10^{-5}	1.04×10^{-4}	1.03×10^{-4}	1.11×10^{-4}	1.14×10^{-4}	$[1.02 \times 10^{-4},$ $1.26 \times 10^{-4}]$
1.1×10^4	4.44×10^{-4}	7.75×10^{-4}	6.73×10^{-4}	7.75×10^{-4}	7.69×10^{-4}	$[7.38 \times 10^{-4},$ $8.01 \times 10^{-4}]$
1.2×10^4	9.43×10^{-4}	1.68×10^{-3}	1.44×10^{-3}	1.68×10^{-3}	1.63×10^{-3}	$[1.58 \times 10^{-3},$ $1.68 \times 10^{-3}]$
1.4×10^4	3.30×10^{-3}	5.83×10^{-3}	5.06×10^{-3}	5.83×10^{-3}	5.66×10^{-3}	$[5.58 \times 10^{-3},$ $5.75 \times 10^{-3}]$
1.6×10^4	8.93×10^{-3}	0.0150	0.0136	0.0150	0.0151	[0.0150, 0.0153]
1.8×10^4	0.0199	0.0315	0.0298	0.0339	0.0330	[0.0328, 0.0332]
2.0×10^4	0.0385	0.0570	0.0557	0.0616	0.0615	[0.0613, 0.0618]
2.2×10^4	0.0662	0.0925	0.0923	0.1005	0.1018	[0.1014, 0.1021]
2.4×10^4	0.1037	0.1386	0.1387	0.1505	0.1534	[0.1530, 0.1538]
2.6×10^4	0.1507	0.1948	0.1928	0.2092	0.2148	[0.2144, 0.2153]
2.8×10^4	0.2058	0.2598	0.2516	0.2725	0.2830	[0.2824, 0.2835]

| 3.0×10^4 | 0.2670 | 0.3306 | 0.3120 | 0.3385 | 0.3550 | [0.3545, 0.3555] |

Table 4 Percentage of error under different failure levels

Limit State	Error (%)			
	FORM	Improved FORM	SORM	Improved SORM
0.8×10^4	30.42	9.32	2.23	3.70
0.9×10^4	39.72	8.80	10.29	2.87
1.1×10^4	42.30	0.72	12.48	0.72
1.2×10^4	42.14	3.29	11.69	3.29
1.4×10^4	41.74	2.97	10.69	2.97
1.6×10^4	41.01	0.77	10.28	0.76
1.8×10^4	39.62	4.74	9.95	2.57
2.0×10^4	37.43	7.44	9.40	0.09
2.2×10^4	34.98	9.11	9.28	1.26
2.4×10^4	32.42	9.68	9.58	1.93
2.6×10^4	29.87	9.31	10.26	2.74
2.8×10^4	27.28	8.19	11.07	3.81
3.0×10^4	24.78	6.89	12.11	4.72
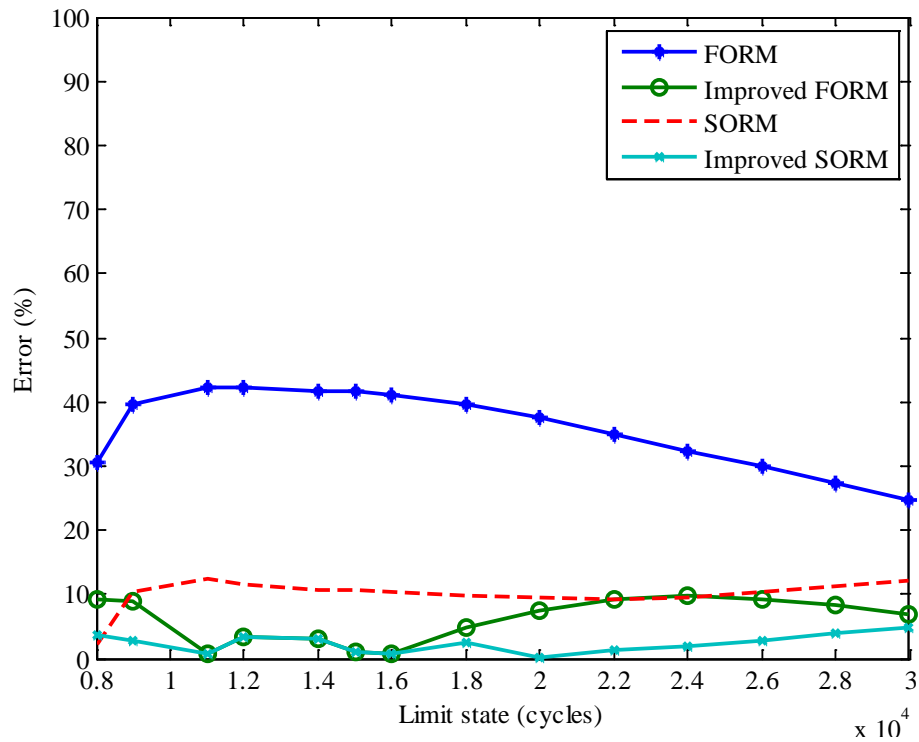
Fig. 6 Percentage error under different failure levels

Table 5 Number of function calls needed under different failure levels

| Limit State	NOF				
	FORM	Improved FORM	SORM	Improved SORM	MCS
0.8×10^4	313	100	404	155	3×10^6
0.9×10^4	287	80	378	135	3×10^6
1.1×10^4	287	80	378	135	3×10^6
1.2×10^4	261	80	352	135	3×10^6
1.4×10^4	261	80	352	135	3×10^6
1.6×10^4	235	80	326	135	3×10^6
1.8×10^4	235	80	326	135	3×10^6
2.0×10^4	209	80	300	135	3×10^6
2.2×10^4	183	100	274	155	3×10^6
2.4×10^4	183	100	274	155	3×10^6
2.6×10^4	157	100	248	155	3×10^6
2.8×10^4	157	80	248	135	3×10^6
3.0×10^4	131	60	222	115	3×10^6
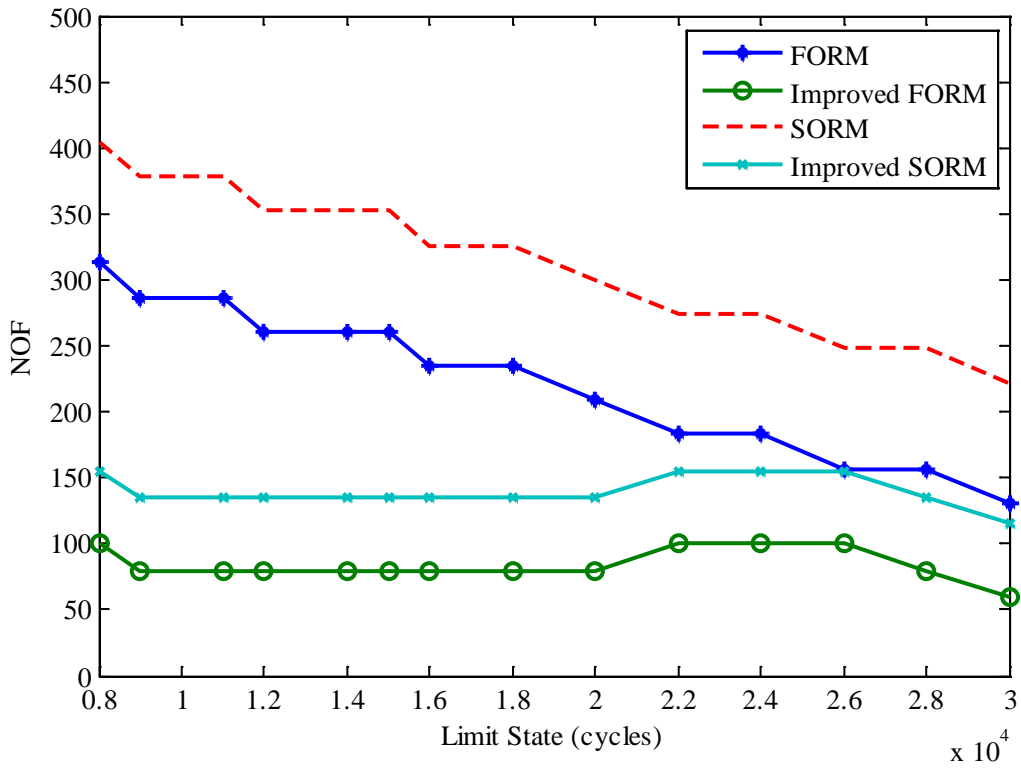
Fig. 7 Function evaluations under different failure levels

The robustness study indicates that the improved FORM and SORM significantly increase the accuracy and efficiency of the direct FORM and SORM, respectively.

6.2. **A door cam**

A door cam, as shown in Figs. 8 and 9, is used to hold the door open while stocking. The fatigue reliability of the cam is to be evaluated during the product development process.

For each cycle of the door opening and closing, the cam experiences two kinds of motion, which are the engagement and disengagement of the shoulder. During the motion cycle, the upper and lower legs of the cam deflect until the shoulder passes the gap between the two legs. Figs. 10 and 11 show the working positions and force analysis for the engagement and disengagement of the cam, respectively.
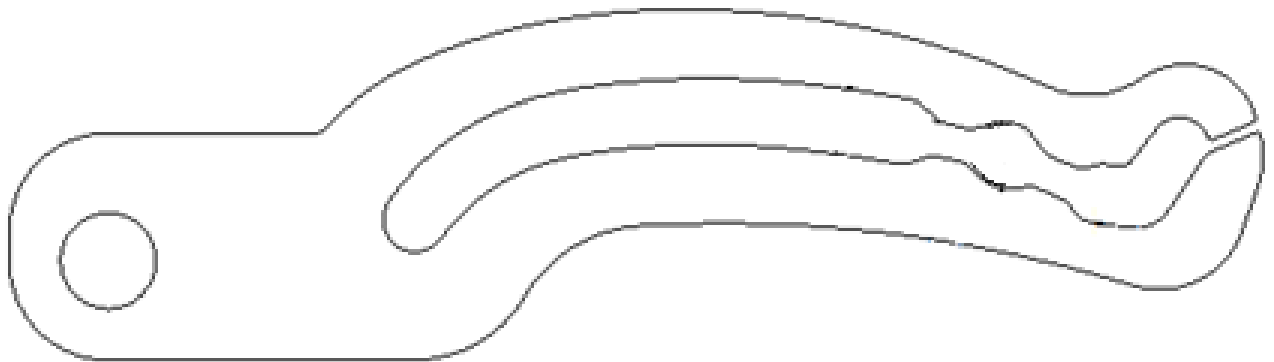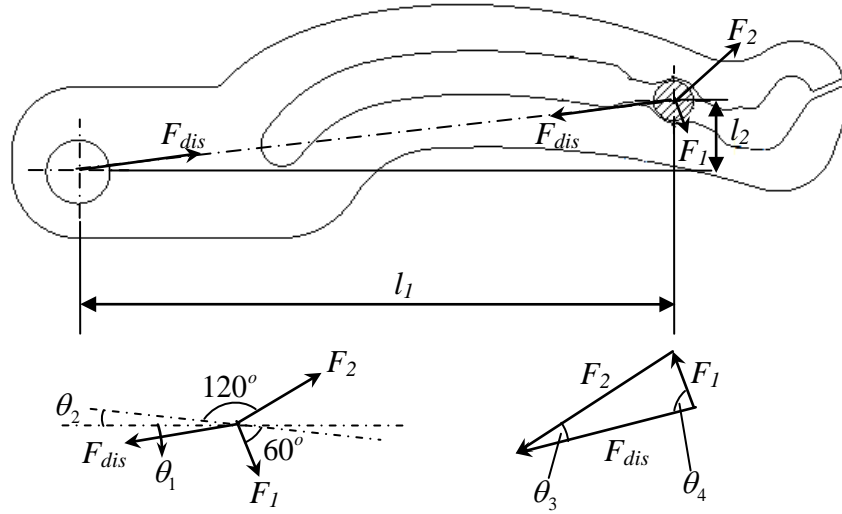
Fig. 8. A door cam
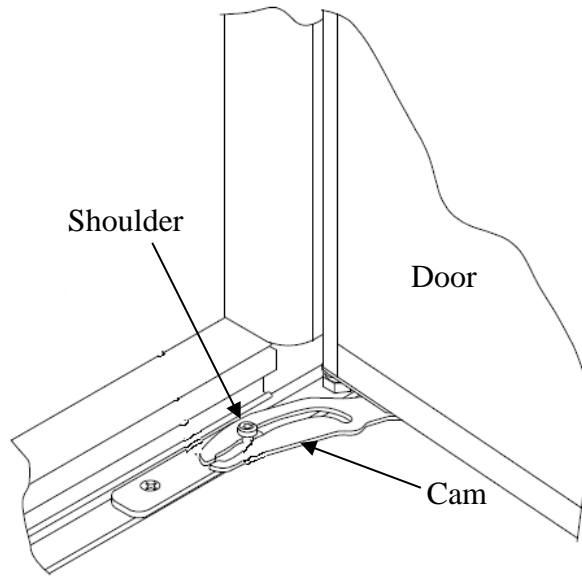
Fig. 9 Door cam and door
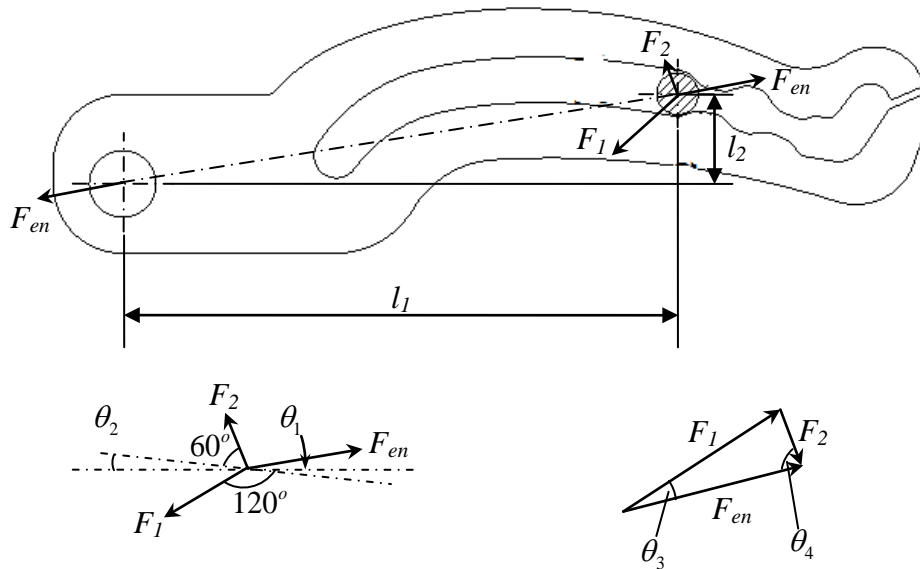
Fig. 10. Working position of the shoulder and force analysis for the engagement

Fig. 11. Working position of the shoulder and force analysis for the disengagement

Fig. 12 shows the simplified stress history of the corner of the upper leg during cycles of engagement and disengagement. Since the motion trend of the cam is known, the stress response of the cam is also known. For every cycle of motion, we have $\mathbf{S}^o_{max} = [S^o_1, S^o_2]$ and $\mathbf{S}^o_{min} = [0, 0]$.
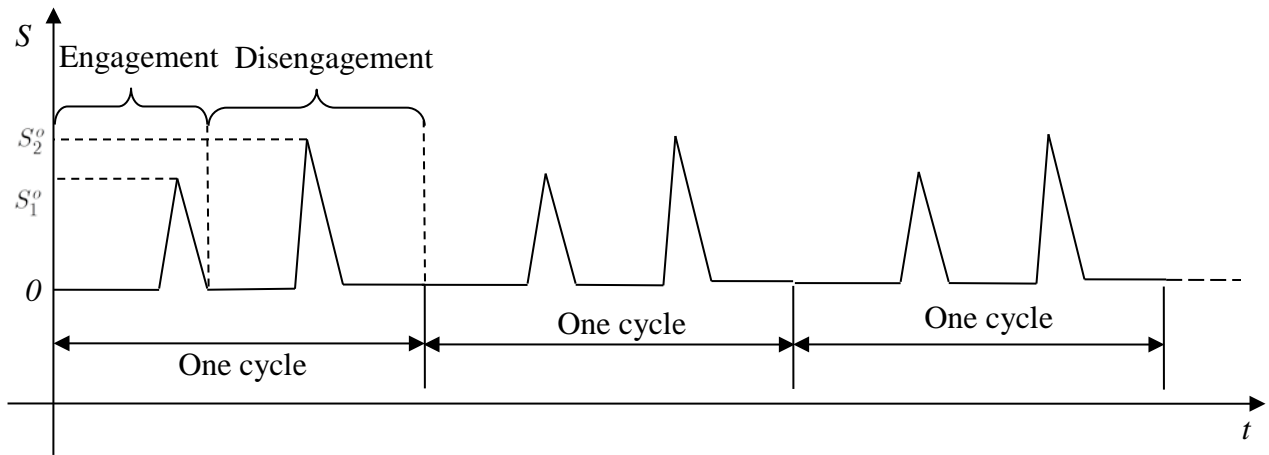
Fig. 12. Stress trend of the corner on the upper leg over cycles

Fig. 12 indicates that the stress history of the cam is characterized by the maximal stresses of engagement and disengagement (i.e. S^o_1 and S^o_2). The force and stress analyses found that the

stress response is dependent upon the open distance d_{open} between the upper and lower legs. The stress responses therefore can be expressed as functions of d_{open}.

d_{open} is a parameter related to the initial gap between two legs and the diameter of the shoulder and is given by

$$d_{open} = d_{sh} - d_{gap} \tag{62}$$

in which d_{sh} is the diameter of the shoulder, and d_{gap} is the initial gap between the two legs.

To explore the relationship between the stress responses and d_{open}, we performed finite element analyses (FEA) based on the force analyses given in Figs. 10 and 11, which result in the following stress responses:

$$S_1^o(d_{open}) = 1.437 \times 10^3 (d_{sh} - d_{gap}) - 0.1021 \tag{63}$$

$$S_2^o(d_{open}) = 1.2 \times 10^3 (d_{sh} - d_{gap}) - 0.5 \tag{64}$$

Two snapshots of the stress distribution under engagement and disengagement of the cam obtained from FEA are given in Figs. 13 and 14.

The cam is made of brittle material, and the Goodman correction was made as well. The corrected stress responses, S_i, $i = 1, 2$ are given by

$$S_i = \frac{S_i^o(d_{open})S_u}{2S_u - S_i^o(d_{open})} \tag{65}$$

Due to manufacturing imprecision, the initial gap d_{gap} and the diameter of the shoulder d_{sh} are random. But we treat d_{sh} as deterministic because its randomness is negligible compared with that of d_{gap}. Also considering variations in the ultimate tensile strength of the material, we have two random variables d_{gap} and S_u in the stress response function. According to the stress

response analysis given in Fig. 12, there are also two random variables in the fatigue life analysis model.
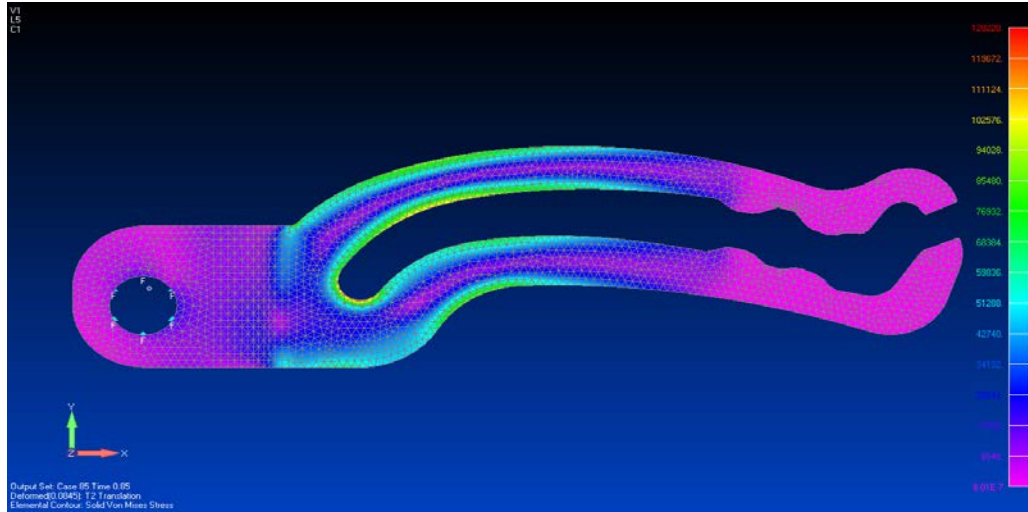
Fig. 13. One snapshot of stress distribution under engagement motion
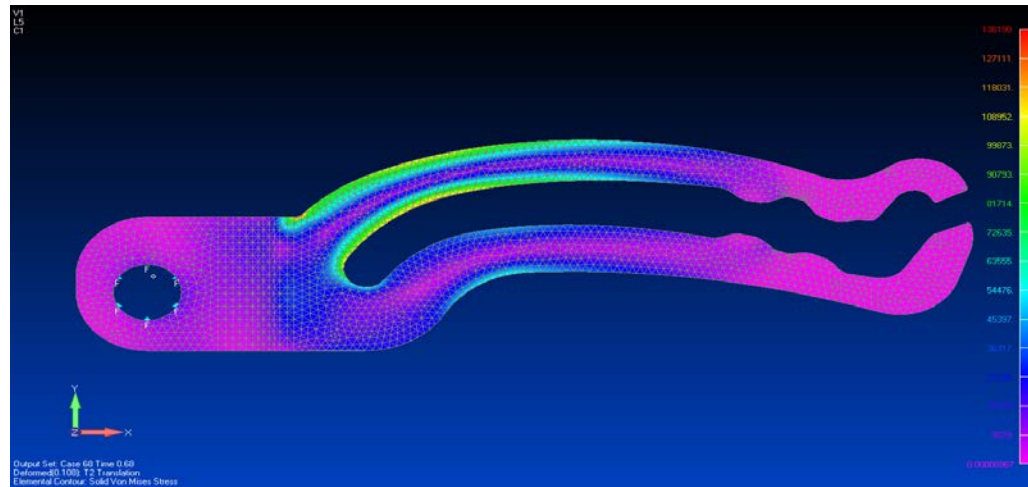
Fig. 14. One snapshot of stress distribution under disengagement motion

The number of cycles to failure follows a Lognormal distributions with mean value of

$$\mu_{\log(N)} = \log\{10^{[12.2-3.68\log_{10}(S_i)]}\} \tag{66}$$

and standard deviation of

$$\sigma_{\log(N)} = 0.03 \mu_{\log(N)} \tag{67}$$

In this example, $d_{sh} = 0.187$ in , and the target fatigue life is $l = 2 \times 10^4$ cycles. Table 6 provides all the random variables needed for the analysis.

Table 6 Random variables of example 2

Variable	Mean Value	Standard Deviation	Distribution Type
d_{gap} (in)	0.107	0.009	Normal
S_u (ksi)	221.7	5	Lognormal

The probability of fatigue failure of the cam was computed by the direct FORM, SORM, the improved FORM, the improved SORM, and MCS. The numbers of samples of MCS was 1×10^6. Results are given in Table 7.

Table 7 Results of reliability analysis

Method	FORM	Improved FORM	SORM	Improved SORM	MCS	
$p_f (\times 10^{-4})$	6.53	7.70	7.55	7.82	8.16	[7.84, 8.48]
Error (%)	19.96	5.61	7.53	4.15	-	
NOF	142	32	157	42	1×10^6	

The results also confirm that the proposed method is more accurate and efficient than the direct use of FORM and SORM.

7. Conclusion

33

It is important to account for the stress-dependent characteristics of material fatigue properties for fatigue reliability analysis. Directly using the First Order Reliability Method (FORM) or Second Order Reliability Method (SORM) for the analysis may not be efficient and may produce large errors in the predicted fatigue reliability as shown in the examples. The accuracy, as well as the efficiency, can be improved with the proposed method that integrates the saddlepoint approximation and the conditional fatigue reliability analysis.

The new method can predict the fatigue reliability or the probability distribution of the fatigue life for structures under cyclic loadings with known trend. This assumption holds for many applications. The method accommodates not only random variables with different distributions in the input variables to stress response functions, as well as uncertain parameters in the S-N curve.

Acknowledgement

References

[1] Correia, J. a. F. O., De Jesus, A. M. P., and Fernández-Canteli, A., 2013, "Local Unified Probabilistic Model for Fatigue Crack Initiation and Propagation: Application to a Notched Geometry," Engineering Structures, 52, pp. 394-407.
[2] Zhang, D. K., Geng, H., Zhang, Z. F., Wang, D. G., Wang, S. Q., and Ge, S. R., 2013, "Investigation on the Fretting Fatigue Behaviors of Steel Wires under Different Strain Ratios," Wear, 303(1-2), pp. 334-342.
[3] Asi, O., and Yeşil, T., 2013, "Failure Analysis of an Aircraft Nose Landing Gear Piston Rod End," Engineering Failure Analysis, 32, pp. 283-291.
[4] Sousa, C., Rocha, J. F., Calçada, R., and Serra Neves, A., 2013, "Fatigue Analysis of Box-Girder Webs Subjected to in-Plane Shear and Transverse Bending Induced by Railway Traffic," Engineering Structures, 54, pp. 248-261.

[5] Lee, Y. J., and Song, J., 2012, "Finite-Element-Based System Reliability Analysis of Fatigue-Induced Sequential Failures," Reliability Engineering and System Safety, 108, pp. 131-141.

[6] Li, F. Z., and Low, Y. M., 2012, "Fatigue Reliability Analysis of a Steel Catenary Riser at the Touchdown Point Incorporating Soil Model Uncertainties," Applied Ocean Research, 38, pp. 100-110.

[7] Rathod, V., Yadav, O. P., Rathore, A., and Jain, R., 2012, "Reliability-Based Design Optimization Considering Probabilistic Degradation Behavior," Quality and Reliability Engineering International, 28(8), pp. 911-923.

[8] Beck, A. T., and Gomes, W. J. D. S., 2013, "Stochastic Fracture Mechanics Using Polynomial Chaos," Probabilistic Engineering Mechanics, 34, pp. 26-39.

[9] Chan, K. S., Enright, M. P., Moody, J. P., Hocking, B., and Fitch, S. H. K., 2012, "Life Prediction for Turbopropulsion Systems under Dwell Fatigue Conditions," Journal of Engineering for Gas Turbines and Power, 134(12), pp. 122501 (8 pages).

[10] Larsen, J. M., Jha, S. K., Szczepanski, C. J., Caton, M. J., John, R., Rosenberger, A. H., Buchanan, D. J., Golden, P. J., and Jira, J. R., 2013, "Reducing Uncertainty in Fatigue Life Limits of Turbine Engine Alloys," International Journal of Fatigue, pp.103-112.

[11] Guo, T., and Chen, Y. W., 2013, "Fatigue Reliability Analysis of Steel Bridge Details Based on Field-Monitored Data and Linear Elastic Fracture Mechanics," Structure and Infrastructure Engineering, 9(5), pp. 496-505.

[12] Liu, Y., and Mahadevan, S., 2009, "Efficient Methods for Time-Dependent Fatigue Reliability Analysis," AIAA Journal, 47(3), pp. 494-504.

[13] Low, Y. M., 2013, "A New Distribution for Fitting Four Moments and Its Applications to Reliability Analysis," Structural Safety, 42, pp. 12-25.

[14] Huang, W., Wang, T. J., Garbatov, Y., and Guedes Soares, C., 2013, "Dfr Based Fatigue Reliability Assessment of Riveted Lap Joint Accounting for Correlations," International Journal of Fatigue, 47, pp. 106-114.

[15] Rajaguru, P., Lu, H., and Bailey, C., 2012, "Application of Kriging and Radial Basis Function in Power Electronic Module Wire Bond Structure Reliability under Various Amplitude Loading," International Journal of Fatigue, 45, pp. 61-70.

[16] Baumert, E. K., and Pierron, O. N., 2012, "Fatigue Properties of Atomic-Layer-Deposited Alumina Ultra-Barriers and Their Implications for the Reliability of Flexible Organic Electronics," Applied Physics Letters, 101(25), pp. 251901

[17] Norouzi, M., and Nikolaidis, E., 2012, "Efficient Method for Reliability Assessment under High-Cycle Fatigue," International Journal of Reliability, Quality and Safety Engineering, 19(5), pp. 1250022 (27 pages).

[18] Wei, Z., Yang, F., Lin, B., Luo, L., Konson, D., and Nikbin, K., 2013, "Deterministic and Probabilistic Creep-Fatigue-Oxidation Crack Growth Modeling," Probabilistic Engineering Mechanics, 33, pp. 126-134.

[19] Hasan, S. M., Khan, F., and Kenny, S., 2012, "Probabilistic Transgranular Stress Corrosion Cracking Analysis for Oil and Gas Pipelines," Journal of Pressure Vessel Technology, Transactions of the ASME, 134(5), pp. 051701 (9 pages).

[20] Jha, S. K., John, R., and Larsen, J. M., 2013, "Incorporating Small Fatigue Crack Growth in Probabilistic Life Prediction: Effect of Stress Ratio in Ti-6al-2sn-4zr-6mo," International Journal of Fatigue, pp.83-95.

[21] Lee, D., Kim, S., Sung, K., Park, J., Lee, T., and Huh, S., 2013, "A Study on the Fatigue Life Prediction of Tire Belt-Layers Using Probabilistic Method," Journal of Mechanical Science and Technology, 27(3), pp. 673-678.

[22] Bengtsson, A., and Rychlik, I., 2009, "Uncertainty in Fatigue Life Prediction of Structures Subject to Gaussian Loads," Probabilistic Engineering Mechanics, 24(2), pp. 224-235.

[23] Wei, Z., Yang, F., Cheng, H., and Nikbin, K., 2011, "Probabilistic Prediction of Crack Growth Based on Creep/Fatigue Damage Accumulation Mechanism," eds., 1539 STP, pp. 230-252.

[24] Wei, Z., Yang, F., Cheng, H., and Nikbin, K., 2011, "Probabilistic Prediction of Crack Growth Based on Creep/Fatigue Damage Accumulation Mechanism," Journal of ASTM International, 8(5), pp. JAI103690 (15 pages).

[25] Xu, Y. L., Chen, Z. W., and Xia, Y., 2012, "Fatigue Assessment of Multi-Loading Suspension Bridges Using Continuum Damage Model," International Journal of Fatigue, 40, pp. 27-35.

[26] Ayala-Uraga, E., and Moan, T., 2007, "Fatigue Reliability-Based Assessment of Welded Joints Applying Consistent Fracture Mechanics Formulations," International Journal of Fatigue, 29(3), pp. 444-456.

[27] Gu, X. K., and Moan, T., 2002, "Long-Term Fatigue Damage of Ship Structures under Nonlinear Wave Loads," Marine Technology, 39(2), pp. 95-104.

[28] Kam, T. Y., Chu, K. H., and Tsai, S. Y., 1998, "Fatigue Reliability Evaluation for Composite Laminates Via a Direct Numerical Integration Technique," International Journal of Solids and Structures, 35(13), pp. 1411-1423.

[29] Kamiński, M., 2002, "On Probabilistic Fatigue Models for Composite Materials," International Journal of Fatigue, 24(2-4), pp. 477-495.

[30] Le, X., and Peterson, M. L., 1999, "Method for Fatigue Based Reliability When the Loading of a Component Is Unknown," International Journal of Fatigue, 21(6), pp. 603-610.

[31] Liao, M., Xu, X., and Yang, Q.-X., 1995, "Cumulative Fatigue Damage Dynamic Interference Statistical Model," International Journal of Fatigue, 17(8), pp. 559-566.

[32] Ni, K., and Zhang, S., 2000, "Fatigue Reliability Analysis under Two-Stage Loading," Reliability Engineering and System Safety, 68(2), pp. 153-158.

[33] Pascual, F. G., and Meeker, W. Q., 1999, "Estimating Fatigue Curves with the Random Fatigue-Limit Model," Technometrics, 41(4), pp. 277-290.

[34] Rowatt, J. D., and Spanos, P. D., 1998, "Markov Chain Models for Life Prediction of Composite Laminates," Structural Safety, 20(2), pp. 117-135.

[35] Liu, Y., and Mahadevan, S., 2007, "Stochastic Fatigue Damage Modeling under Variable Amplitude Loading," International Journal of Fatigue, 29(6), pp. 1149-1161.

[36] Huang, C. Y., Hu, C. K., Yu, C. J., and Sung, C. K., 2013, "Experimental Investigation on the Performance of a Compressed-Air Driven Piston Engine," Energies, 6(3), pp. 1731-1745.

[37] Petrescu, F. I. T., and Petrescu, R. V. V., 2013, "Dynamic Synthesis of the Rotary Cam and Translated Tappet with Roll," International Review on Modelling and Simulations, 6(2), pp. 600-607.

[38] Cihan, K., and Yuksel, Y., 2013, "Deformation of Breakwater Armoured Artificial Units under Cyclic Loading," Applied Ocean Research, 42, pp. 79-86.

[39] Hu, Z., and Du, X., 2012, "Reliability Analysis for Hydrokinetic Turbine Blades," Renewable Energy, 48, pp. 251-262.

[40] Huang, B., and Du, X., 2006, "Uncertainty Analysis by Dimension Reduction Integration and Saddlepoint Approximations," Journal of Mechanical Design, Transactions of the ASME, 128(1), pp. 26-33.

[41] Wen, Y. K., and Chen, H. C., 1987, "On Fast Integration for Time Variant Structural Reliability," Probabilistic Engineering Mechanics, 2(3), pp. 156-162.

[42] Fitzwater, L. M., and Winterstein, S. R., 2001, "Predicting Design Wind Turbine Loads from Limited Data: Comparing Random Process and Random Peak Models," Journal of Solar Energy Engineering, Transactions of the ASME, 123(4), pp. 364-371.

[43] Huang, W., and Moan, T., 2007, "A Practical Formulation for Evaluating Combined Fatigue Damage from High- and Low-Frequency Loads," Journal of Offshore Mechanics and Arctic Engineering, 129(1), pp. 1-8.

[44] Ko, N. H., 2008, "Verification of Correction Factors for Non-Gaussian Effect on Fatigue Damage on the Side Face of Tall Buildings," International Journal of Fatigue, 30(5), pp. 779-792.

[45] Kwon, D. K., and Kareem, A., 2011, "Peak Factors for Non-Gaussian Load Effects Revisited," Journal of Structural Engineering, 137(12), pp. 1611-1619.

[46] Li, J., and Wang, X., 2012, "An Exponential Model for Fast Simulation of Multivariate Non-Gaussian Processes with Application to Structural Wind Engineering," Probabilistic Engineering Mechanics, 30, pp. 37-47.

[47] Cruzado, A., Leen, S. B., Urchegui, M. A., and Gómez, X., 2013, "Finite Element Simulation of Fretting Wear and Fatigue in Thin Steel Wires," International Journal of Fatigue, 55, pp. 7-21.

[48] El Aghoury, I., and Galal, K., 2013, "A Fatigue Stress-Life Damage Accumulation Model for Variable Amplitude Fatigue Loading Based on Virtual Target Life," Engineering Structures, 52, pp. 621-628.

[49] Suyuthi, A., Leira, B. J., and Riska, K., 2013, "Fatigue Damage of Ship Hulls Due to Local Ice-Induced Stresses," Applied Ocean Research, 42, pp. 87-104.

[50] Siddiqui, N. A., and Ahmad, S., 2001, "Fatigue and Fracture Reliability of Tlp Tethers under Random Loading," Marine Structures, 14(3), pp. 331-352.

[51] Aygül, M., Bokesjö, M., Heshmati, M., and Al-Emrani, M., 2013, "A Comparative Study of Different Fatigue Failure Assessments of Welded Bridge Details," International Journal of Fatigue, 49, pp. 62-72.

[52] Wang, X., and Sun, J. Q., 2005, "Effect of Skewness on Fatigue Life with Mean Stress Correction," Journal of Sound and Vibration, 282(3-5), pp. 1231-1237.

[53] Kihl, D. P., and Sarkani, S., 1999, "Mean Stress Effects in Fatigue of Welded Steel Joints," Probabilistic Engineering Mechanics, 14(1-2), pp. 97-104.

[54] Phoon, K. K., Huang, H. W., and Quek, S. T., 2005, "Simulation of Strongly Non-Gaussian Processes Using Karhunen-Loeve Expansion," Probabilistic Engineering Mechanics, 20(2), pp. 188-198.

[55] Phoon, K. K., Huang, S. P., and Quek, S. T., 2002, "Simulation of Second-Order Processes Using Karhunen-Loeve Expansion," Computers and Structures, 80(12), pp. 1049-1060.

[56] Loeve, M., 1977, *Probability Theory. 4th Ed*, Springer, New York.

[57] Goda, K., 2010, "Statistical Modeling of Joint Probability Distribution Using Copula: Application to Peak and Permanent Displacement Seismic Demands," Structural Safety, 32(2), pp. 112-123.

[58] Noh, Y., Choi, K. K., and Du, L., 2009, "Reliability-Based Design Optimization of Problems with Correlated Input Variables Using a Gaussian Copula," Structural and Multidisciplinary Optimization, 38(1), pp. 1-16.

[59] Gupta, A. K., Móri, T. F., and Székely, G. J., 2000, "How to Transform Correlated Random Variables into Uncorrelated Ones," Applied Mathematics Letters, 13(6), pp. 31-33.

[60] Noh, Y., Choi, K. K., and Du, L., 2007, "New Transformation of Dependent Input Variables Using Copula for Rbdo," 7th World Congresses of Structural and Multidisciplinary Optimization, COEX Seoul, 21 May – 25 May 2007, Korea(pp.

[61] Choi, S. K., Grandhi, R. V., and Canfield, R. A., 2007, *Reliability-Based Structural Design*, Springer, New York.

[62] Breitung, K., 1984, "Asymptotic Approximations for Multinormal Integrals," Journal of Engineering Mechanics, 110(3), pp. 357-366.

[63] Kendall, M. G., And Stuart, A.,, 1958, *The Advanced Theory of Statistics Volume1: Distribution Theory*, Charles Griffin & Company, London.